Supplement of Atmos. Chem. Phys., 20, 8953–8973, 2020
https://doi.org/10.5194/acp-20-8953-2020-supplement

Atmospheric Chemistry and Physics
Open Access
EGU

Supplement of

Large difference in aerosol radiative effects from BVOC-SOA treatment in three Earth system models

Moa K. Sporre et al.

Correspondence to: Moa K. Sporre (moa.sporre@nuclear.lu.se)

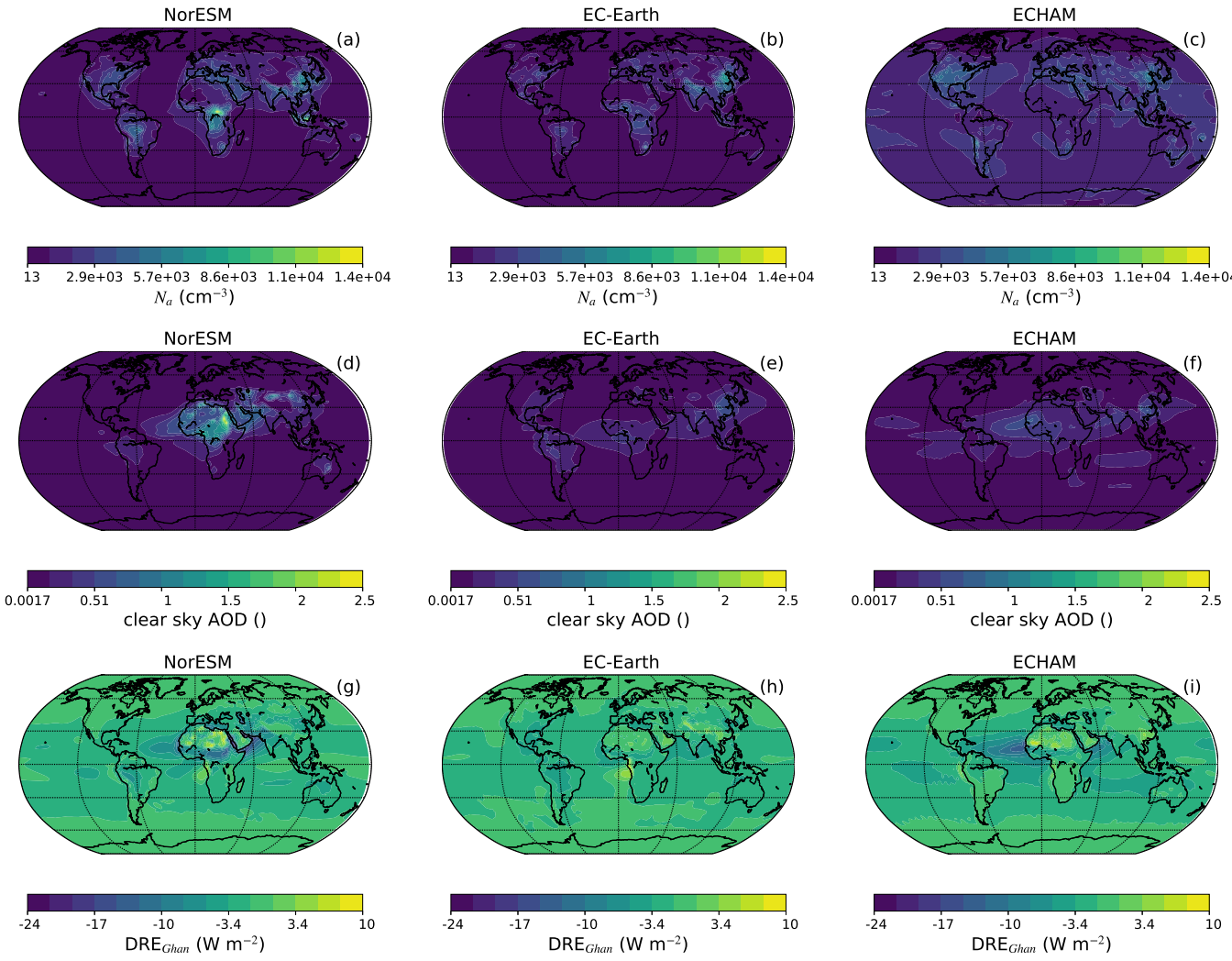

Figure S1. Maps of annually averaged total aerosol number concentration (a-c), clear sky aerosol optical depth (AOD) (d-f) and direct radiative effect (DRE$_{Ghan}$) (g-i) for NorESM, EC-Earth and ECHAM.

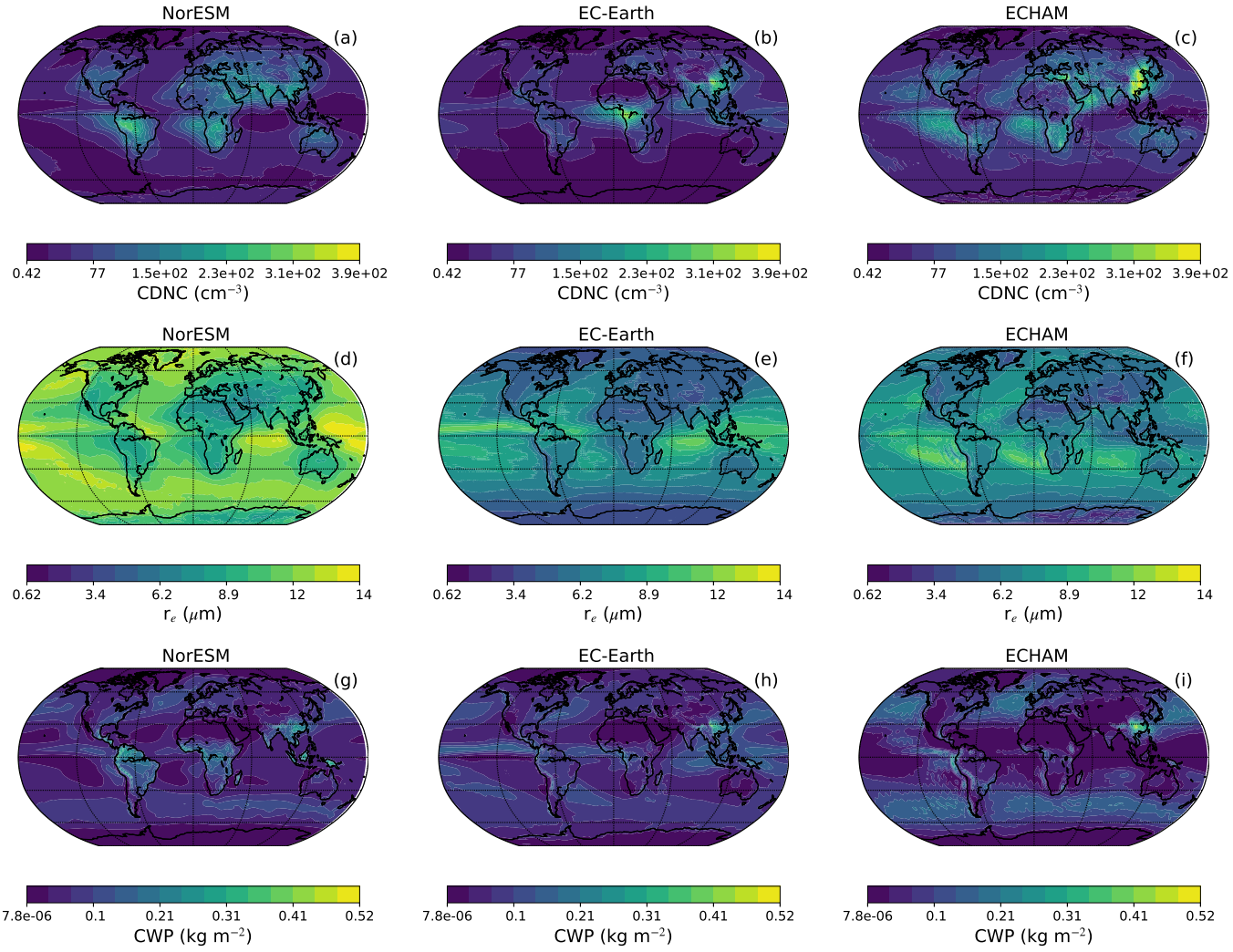

Figure S2. Maps of annually averaged in-cloud droplet number concentration (CDNC) at 860 hPa (a-c), in-cloud effective radius at 860 hPa (r_e) (d-f) and total gridbox cloud water path (CWP) (g-i) for NorESM, EC-Earth and ECHAM.

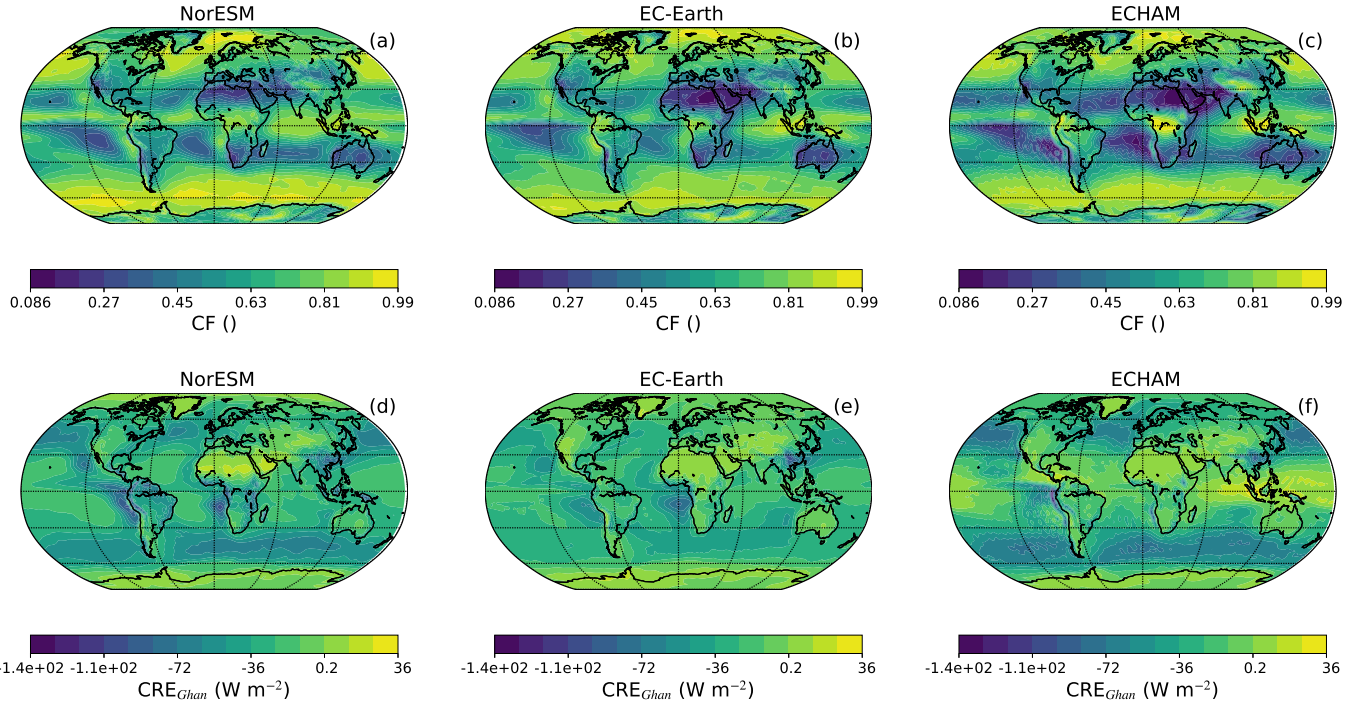

Figure S3. Maps of annually averaged cloud fraction (CF) (a-c) and cloud radiative effects (CRE$_{Ghan}$) (d-f) for NorESM, EC-Earth and ECHAM.

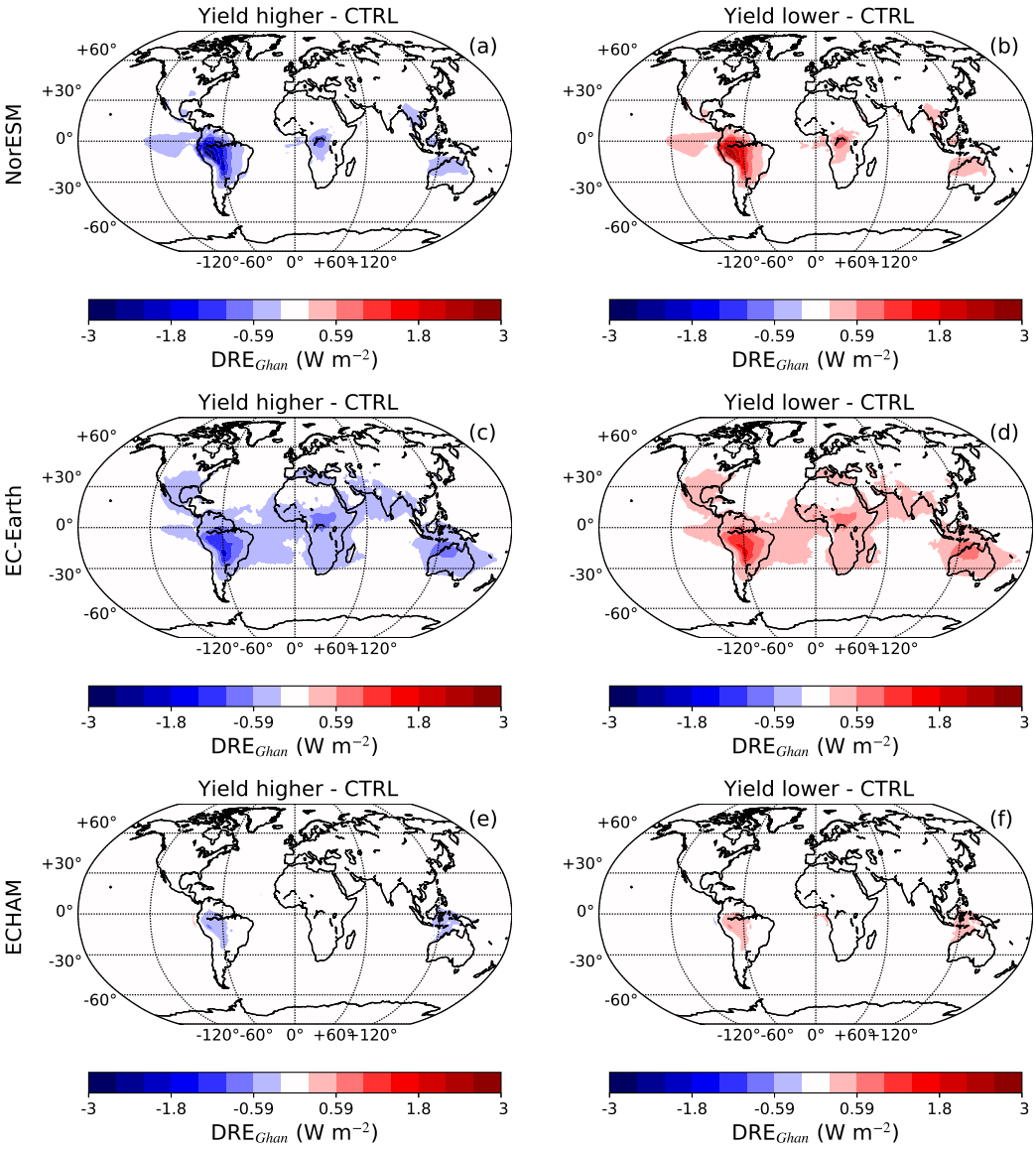

Figure S4. Maps of the difference in the average direct radiative effect (DRE$_{Ghan}$) between the Yield higher (a, c and e) and Yield lower (b, d and f) with respect to the CTRL simulation. This is shown for NorESM (a and b), EC-Earth (c and d) and ECHAM (e and f).

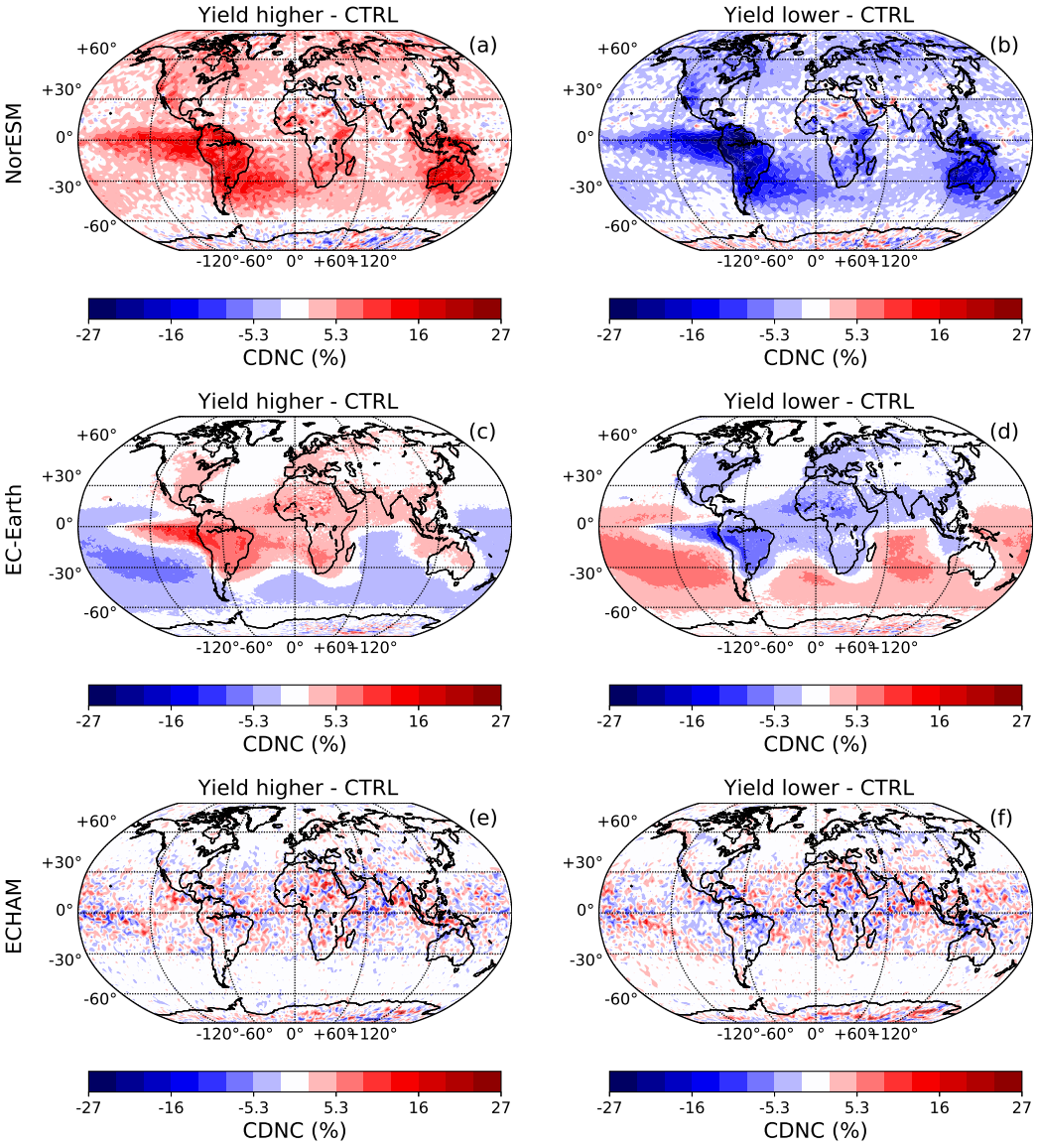

Figure S5. Maps of the difference in the average cloud cloud droplet number concentration (CDNC) between the Yield higher (a, c and e) and Yield lower (b, d and f) with respect to the CTRL simulation. This is shown for NorESM (a and b), EC-Earth (c and d) and ECHAM (e and f).

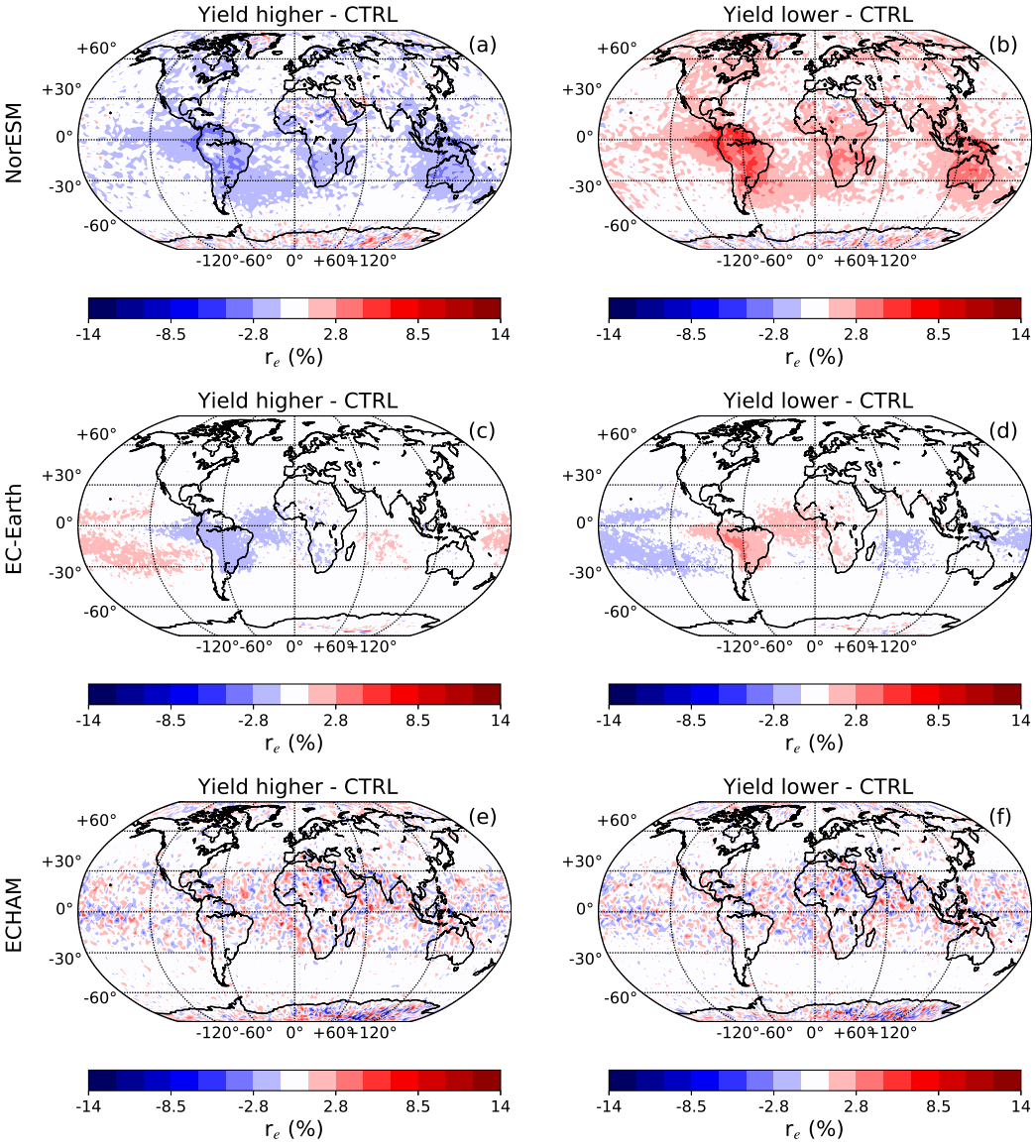

Figure S6. Maps of the difference in the average cloud cloud effective radius (r_e) between the Yield higher (a, c and e) and Yield lower (b, d and f) with respect to the CTRL simulation. This is shown for NorESM (a and b), EC-Earth (c and d) and ECHAM (e and f).

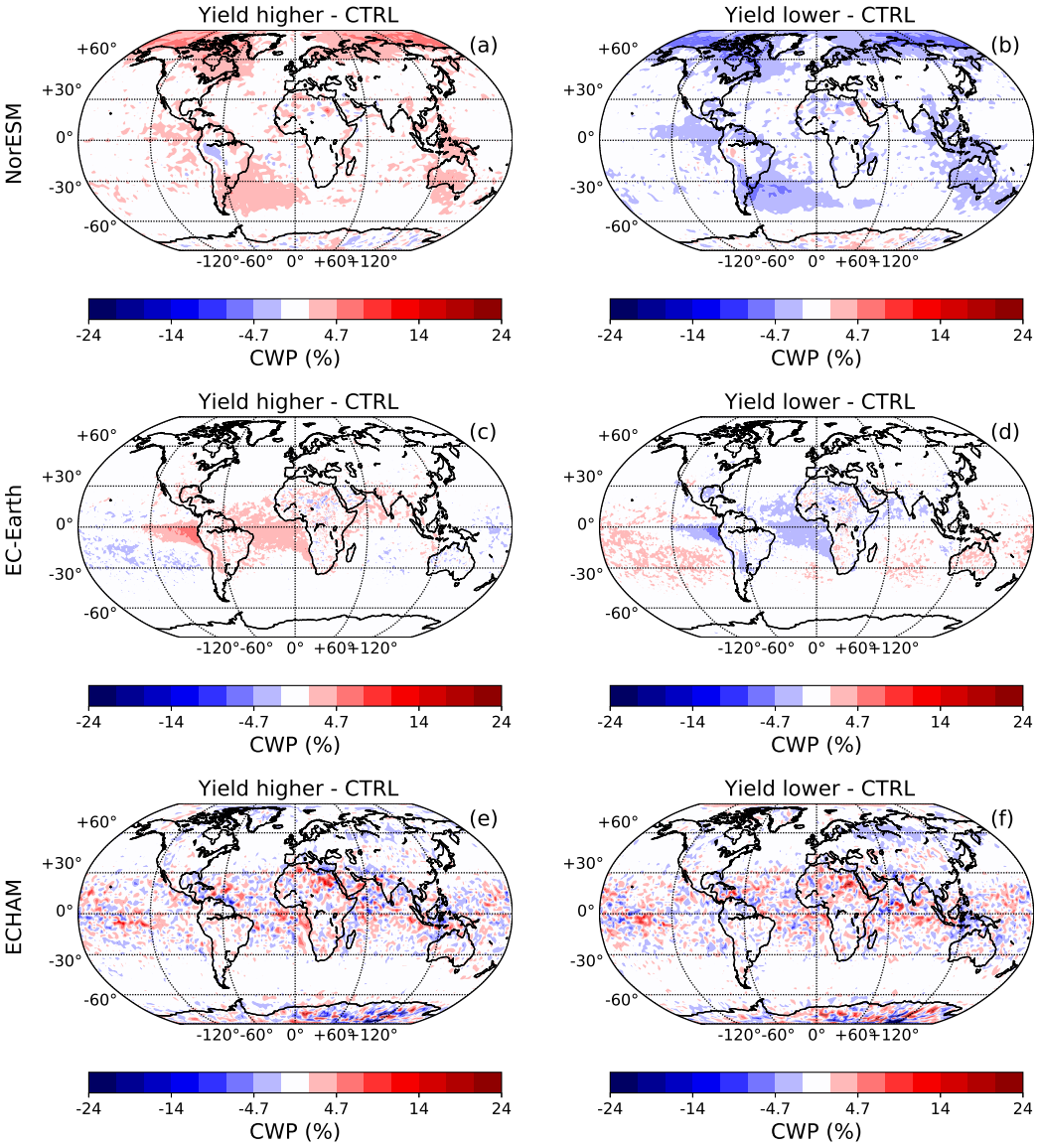

Figure S7. Maps of the difference in the average cloud water path (CWP) between the Yield higher (a, c and e) and Yield lower (b, d and f) with respect to the CTRL simulation. This is shown for NorESM (a and b), EC-Earth (c and d) and ECHAM (e and f).

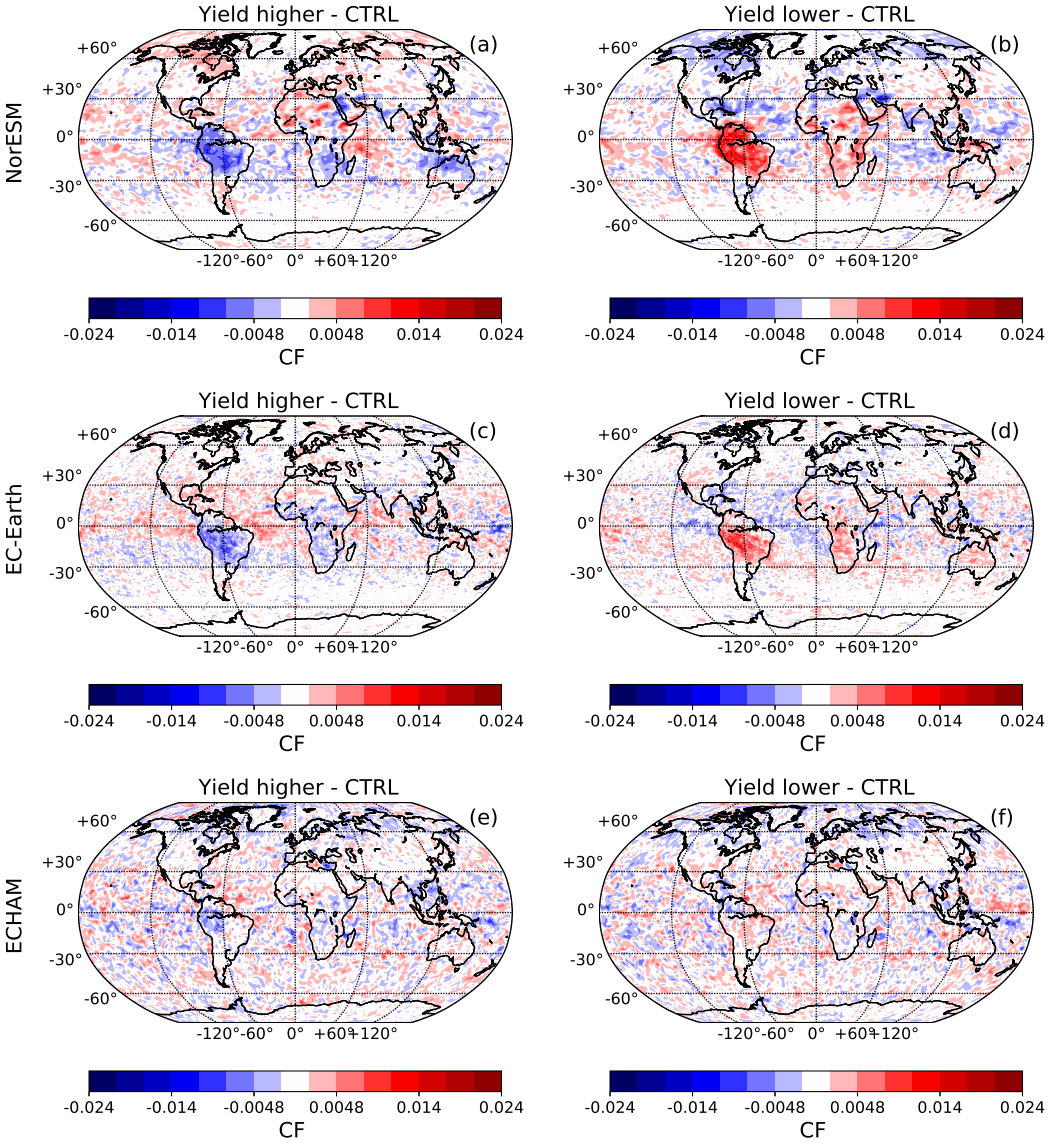

Figure S8. Maps of the difference in the average cloud fraction (CF) between the Yield higher (a, c and e) and Yield lower (b, d and f) with respect to the CTRL simulation. This is shown for NorESM (a and b), EC-Earth (c and d) and ECHAM (e and f).

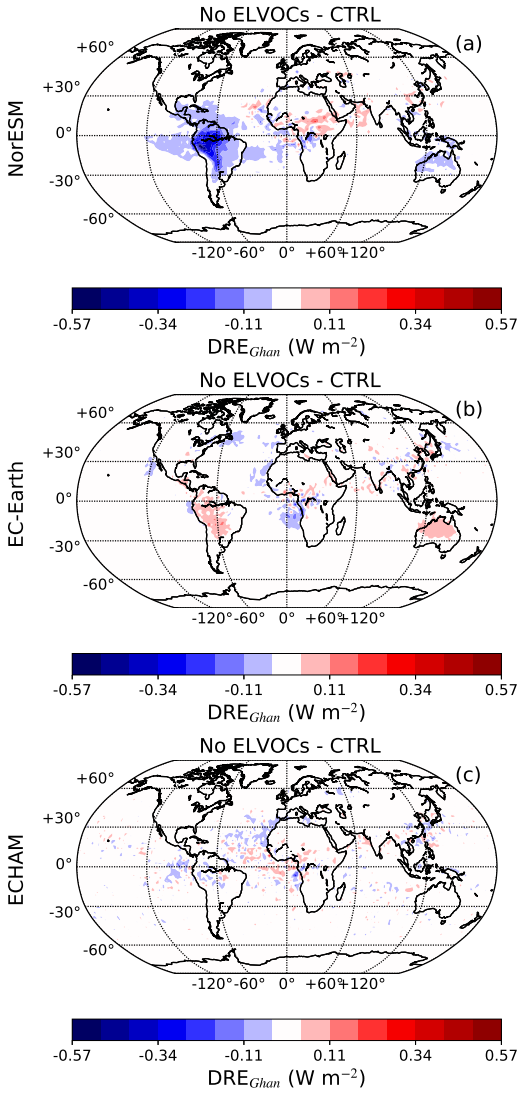

Figure S9. Maps of the difference in the average direct radiative effect (DRE$_{Ghan}$) between the No ELVOCs and the CTRL simulation. This is shown for NorESM (a), EC-Earth (b) and ECHAM (c).

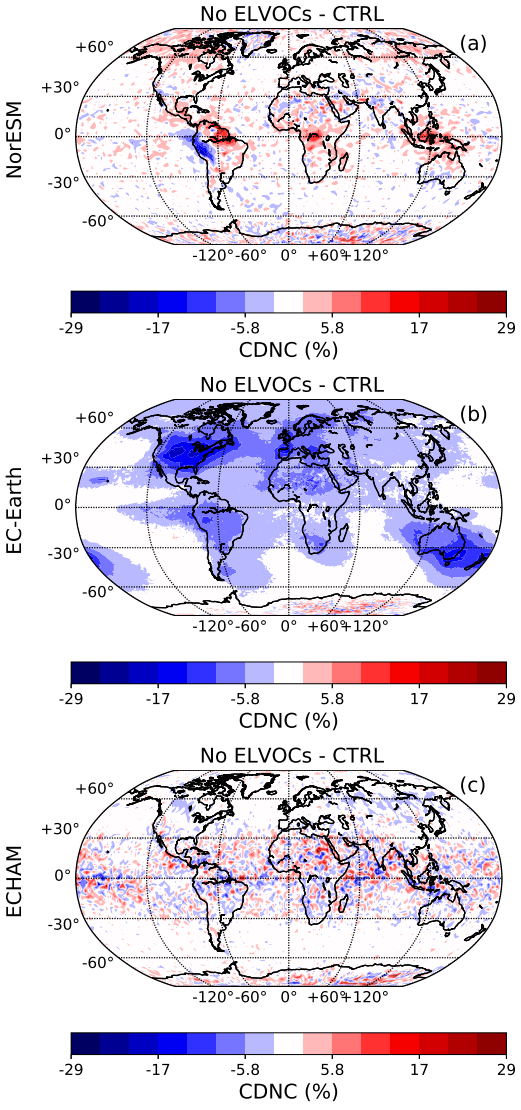

Figure S10. Maps of the difference in the average cloud cloud droplet number concentration (CDNC) between the No ELVOCs and the CTRL simulation. This is shown for NorESM (a), EC-Earth (b) and ECHAM (c).

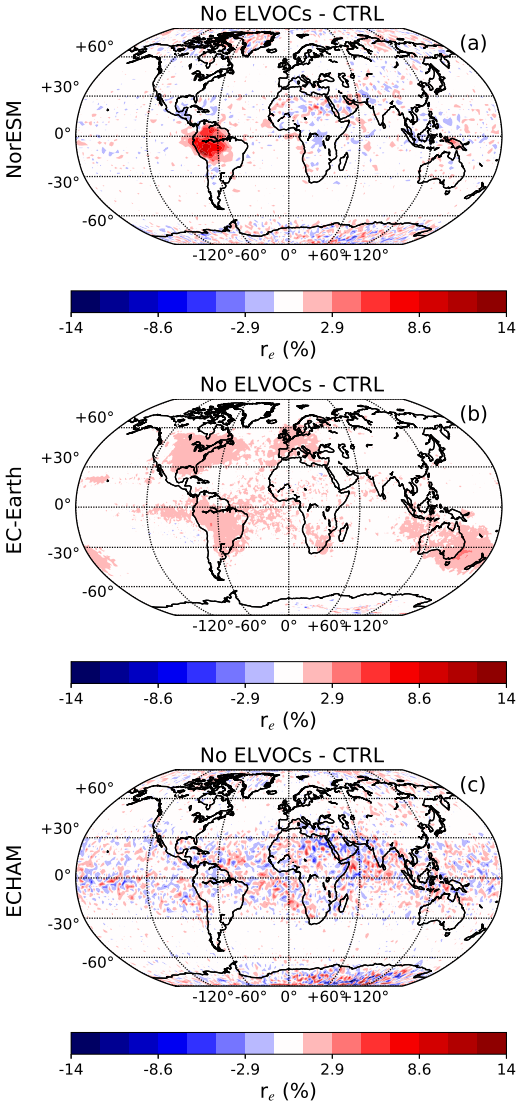

Figure S11. Maps of the difference in the average cloud cloud effective radius (r_e) between the No ELVOCs and the CTRL simulation. This is shown for NorESM (a), EC-Earth (b) and ECHAM (c).

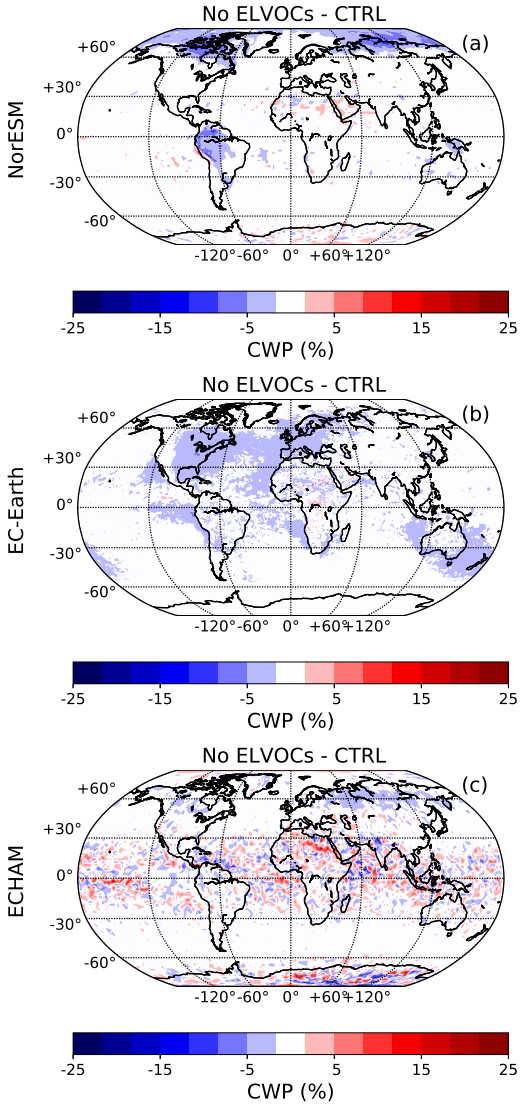

Figure S12. Maps of the difference in the average cloud water path (CWP) between the No ELVOCs and the CTRL simulation. This is shown for NorESM (a), EC-Earth (b) and ECHAM (c).

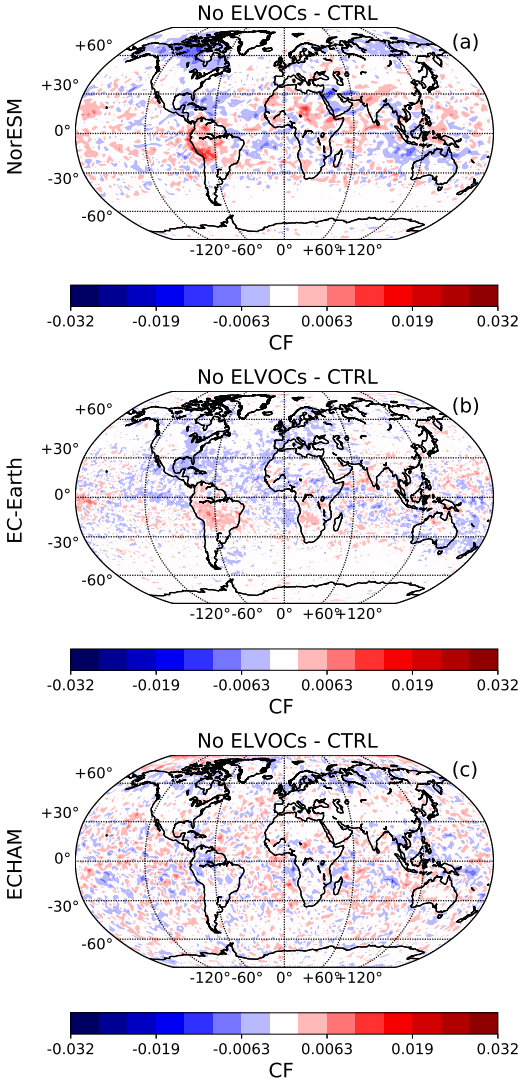

Figure S13. Maps of the difference in the average cloud fraction (CF) between the No ELVOCs and the CTRL simulation. This is shown for NorESM (a), EC-Earth (b) and ECHAM (c).

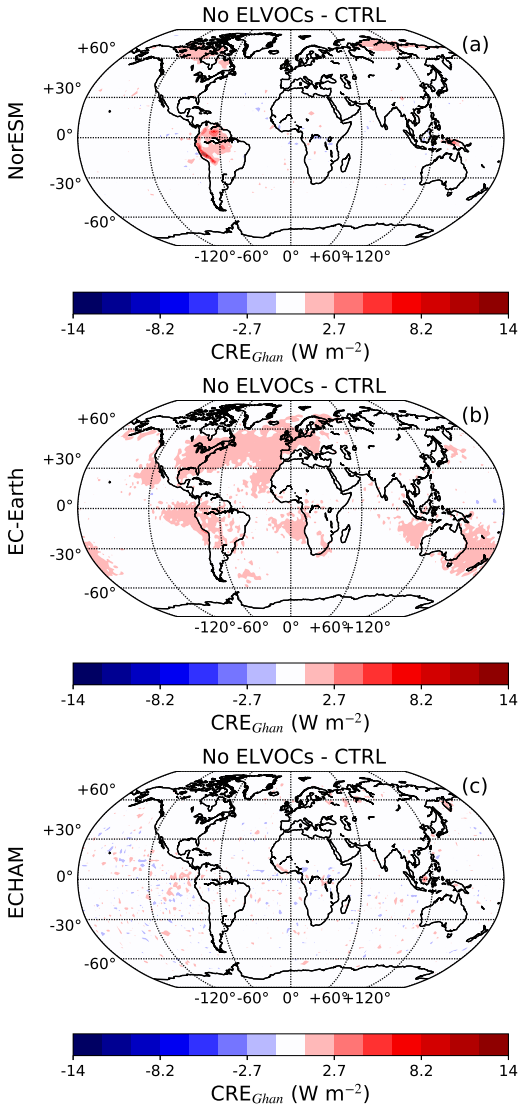

Figure S14. Maps of the difference in the average cloud radiative effect (CRE_{Ghan}) between the No ELVOCs and the CTRL simulation. This is shown for NorESM (a), EC-Earth (b) and ECHAM (c).

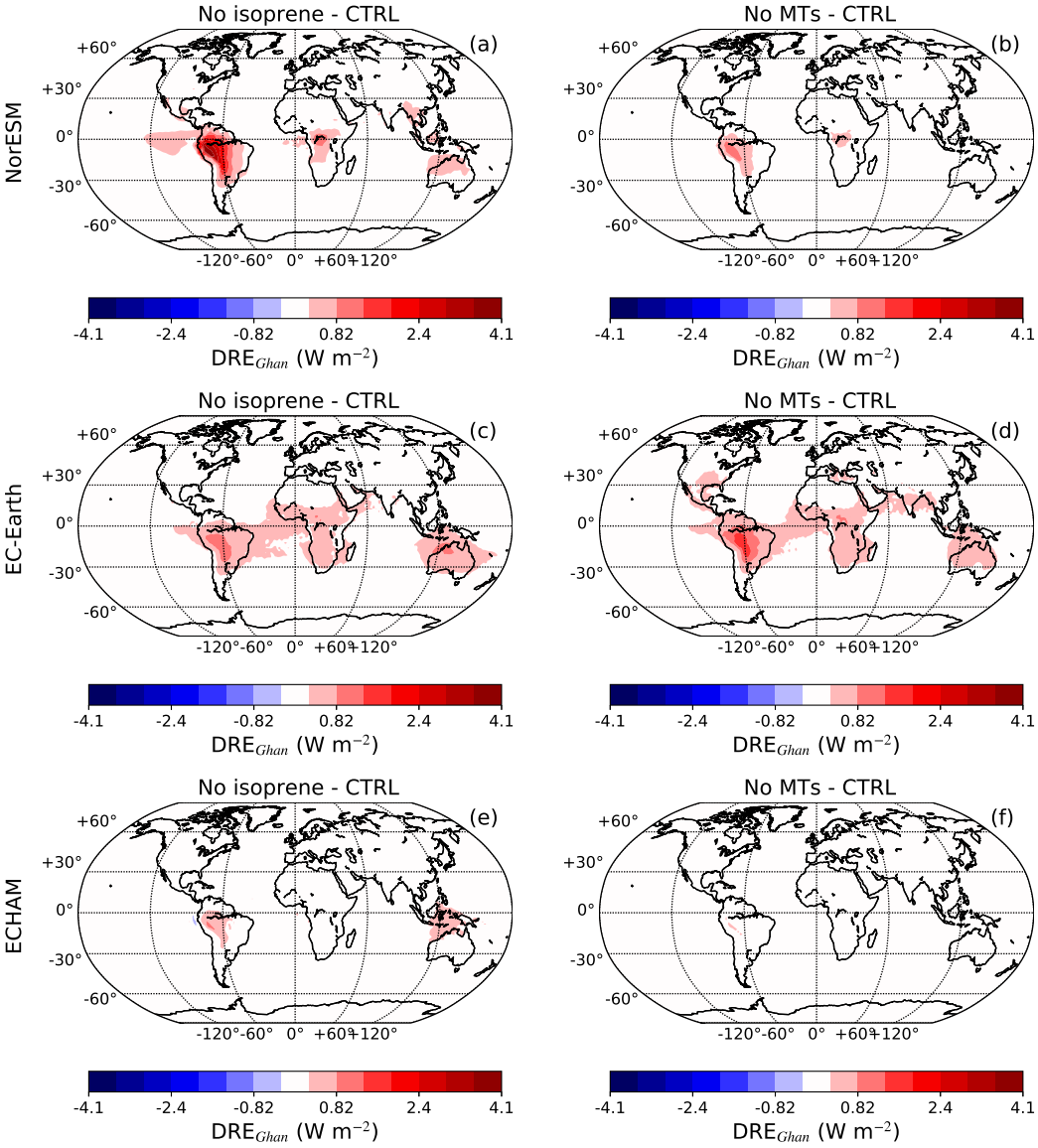

Figure S15. Maps of the difference in the average direct radiative effect (DRE$_{Ghan}$) between the No isoprene (a, c and e) and No MTs (b, d and f) with respect to the CTRL simulation. This is shown for NorESM (a and b), EC-Earth (c and d) and ECHAM (e and f).

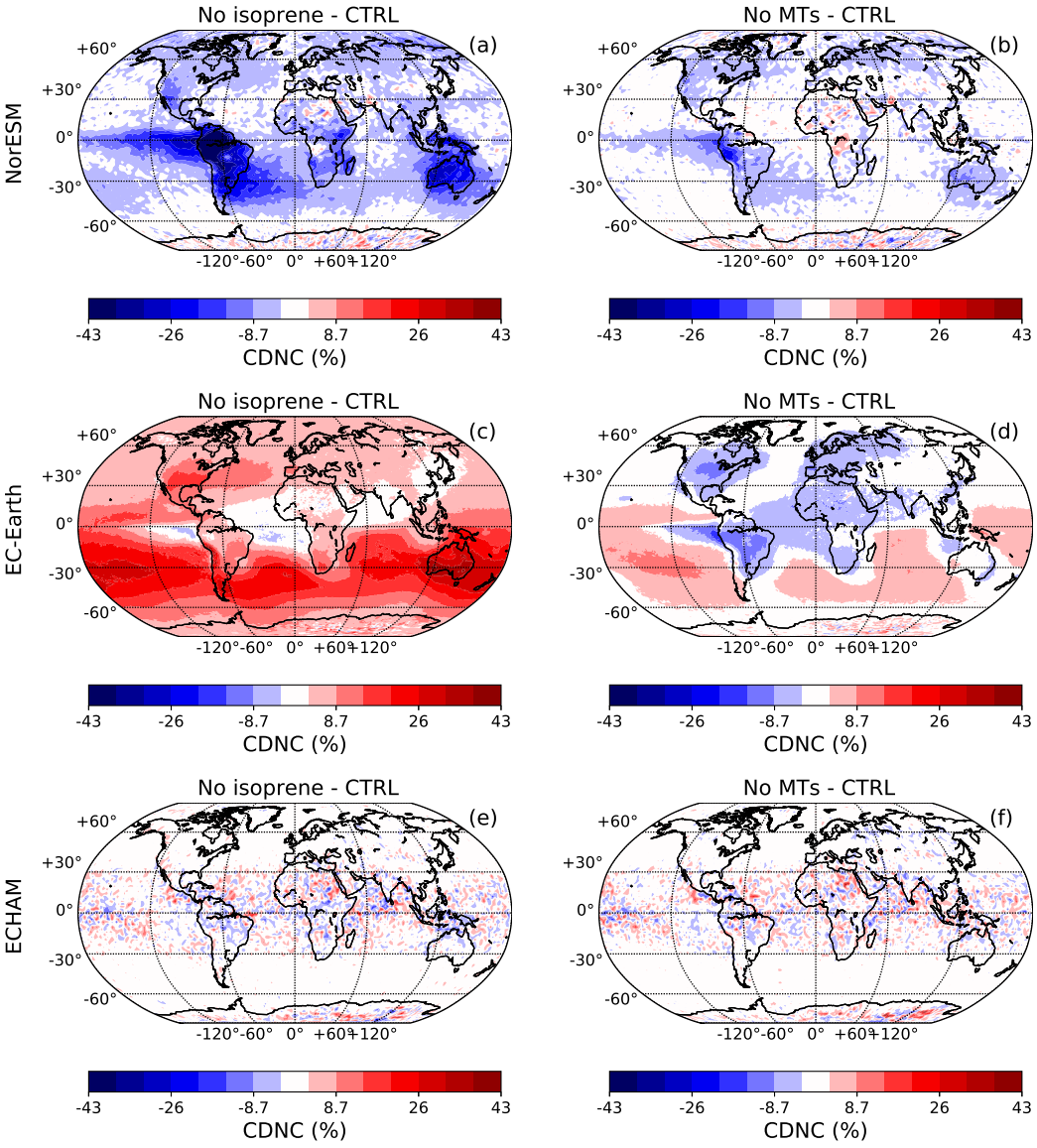

Figure S16. Maps of the difference in the average cloud cloud droplet number concentration (CDNC) between the No isoprene (a, c and e) and No MTs (b, d and f) with respect to the CTRL simulation. This is shown for NorESM (a and b), EC-Earth (c and d) and ECHAM (e and f).

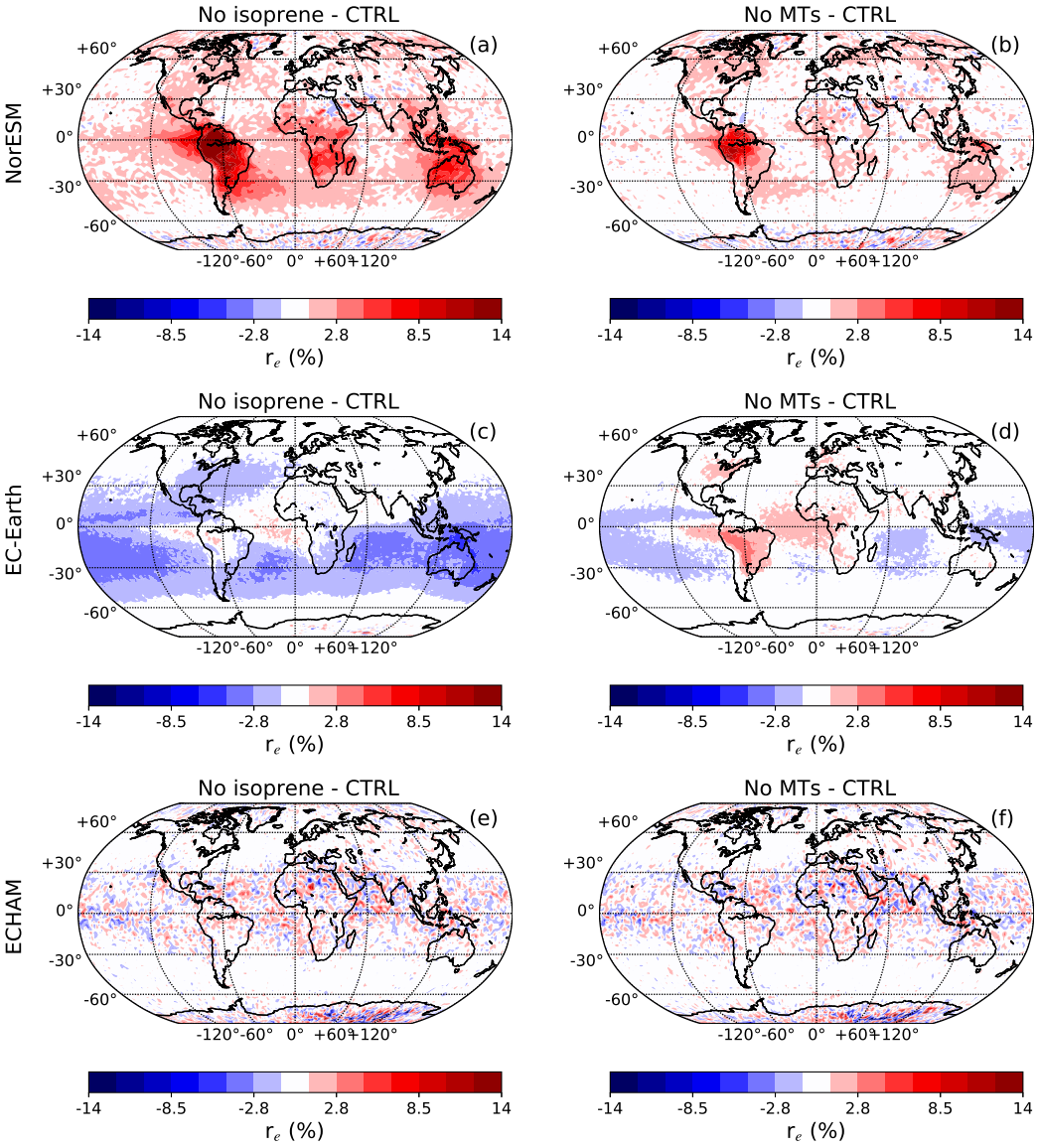

Figure S17. Maps of the difference in the average cloud cloud effective radius (r_e) between the No isoprene (a, c and e) and No MTs (b, d and f) with respect to the CTRL simulation. This is shown for NorESM (a and b), EC-Earth (c and d) and ECHAM (e and f).

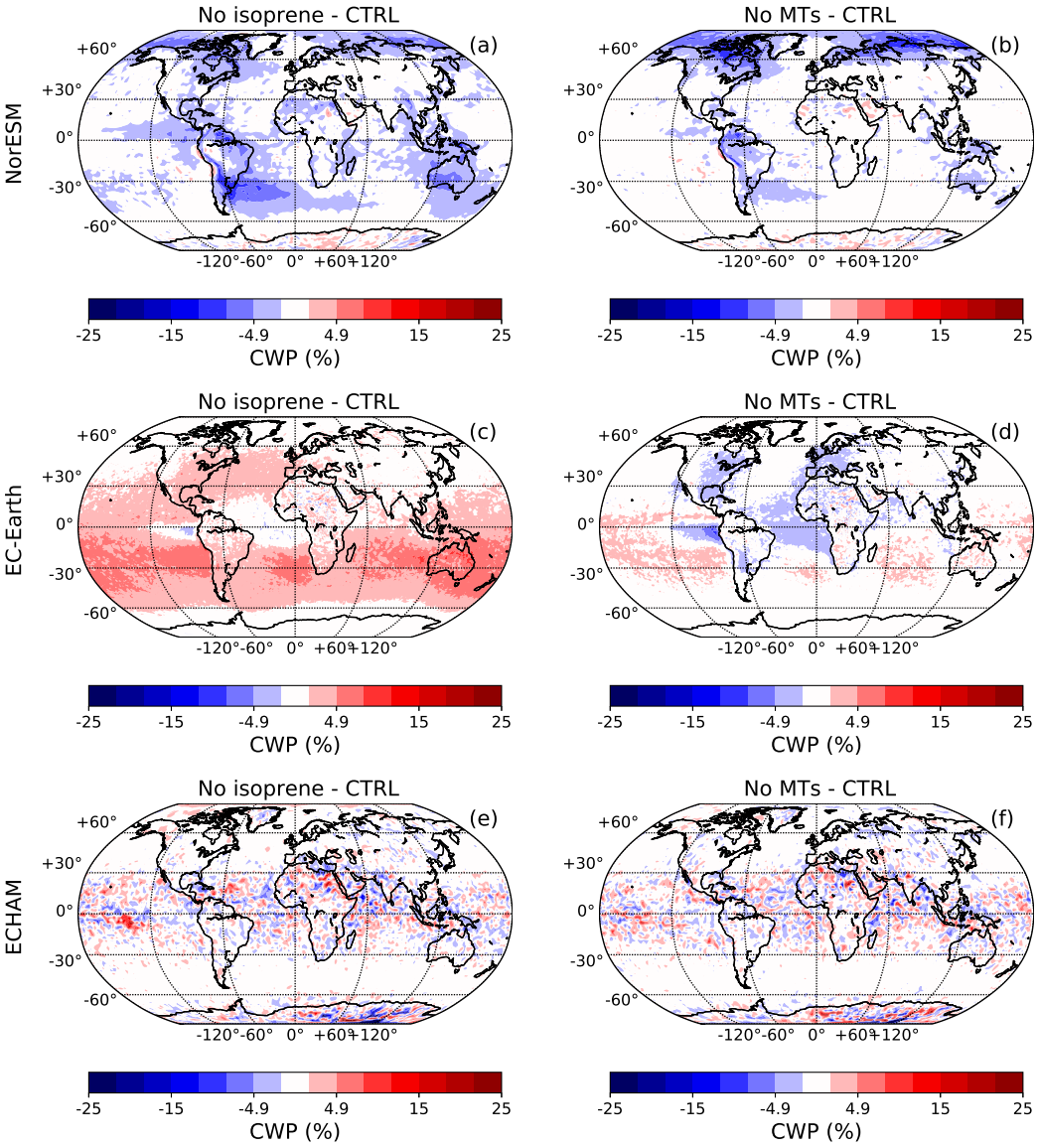

Figure S18. Maps of the difference in the average cloud water path (CWP) between the No isoprene (a, c and e) and No MTs (b, d and f) with respect to the CTRL simulation. This is shown for NorESM (a and b), EC-Earth (c and d) and ECHAM (e and f).

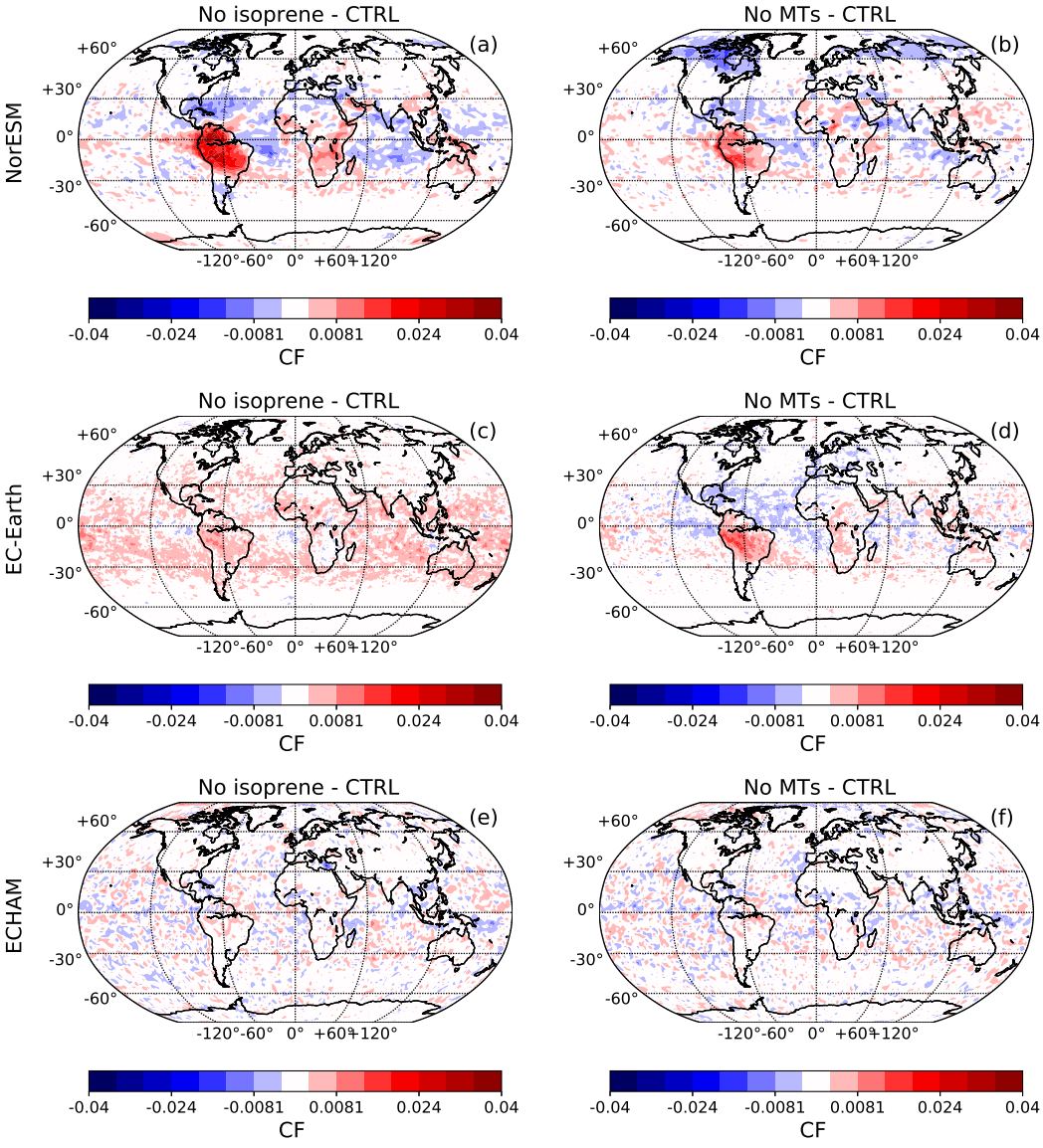

Figure S19. Maps of the difference in the average cloud fraction (CF) between the No isoprene (a, c and e) and No MTs (b, d and f) with respect to the CTRL simulation. This is shown for NorESM (a and b), EC-Earth (c and d) and ECHAM (e and f).

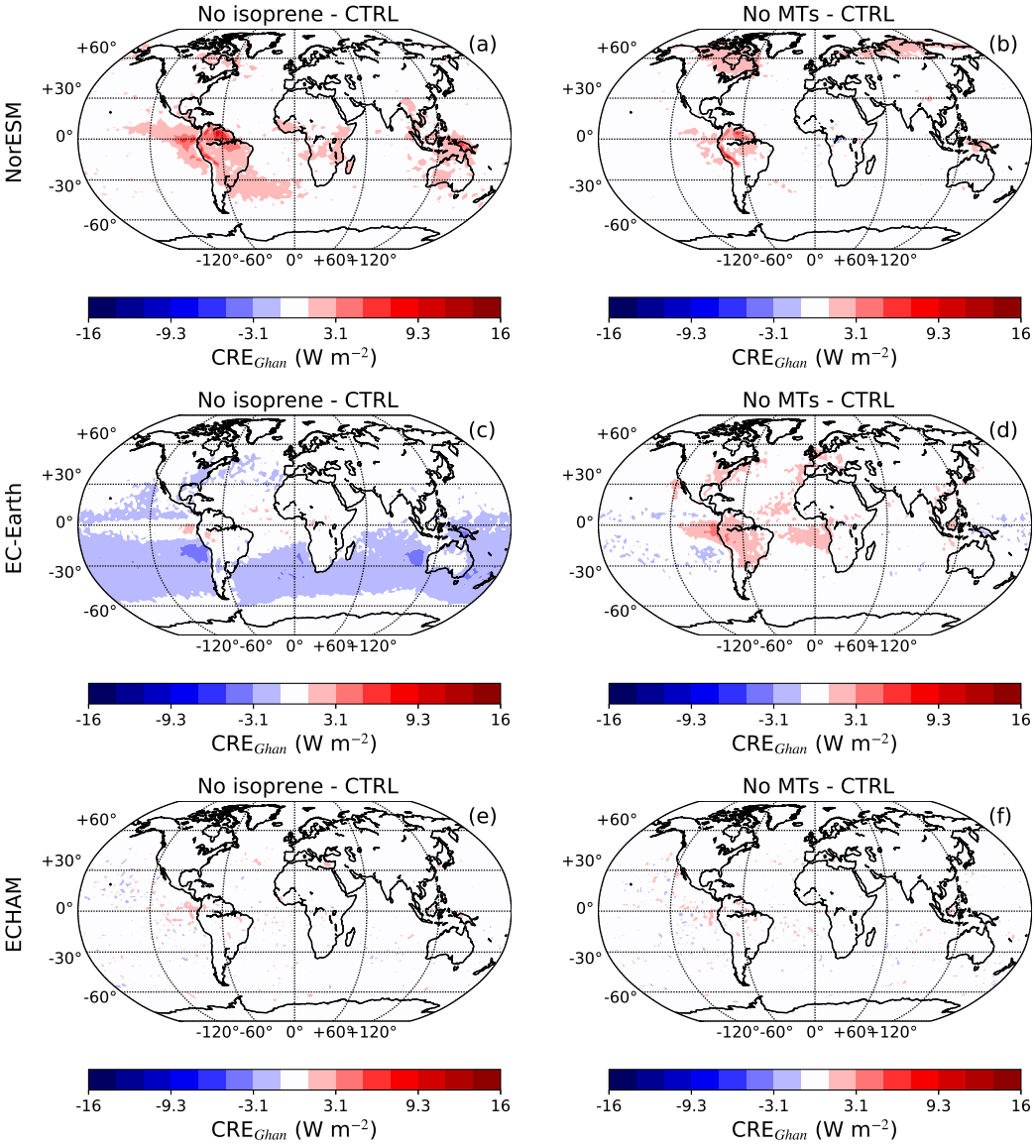

Figure S20. Maps of the difference in the average cloud radiative effect (CRE$_{Ghan}$) between the No isoprene (a, c and e) and No MTs (b, d and f) with respect to the CTRL simulation. This is shown for NorESM (a and b), EC-Earth (c and d) and ECHAM (e and f).

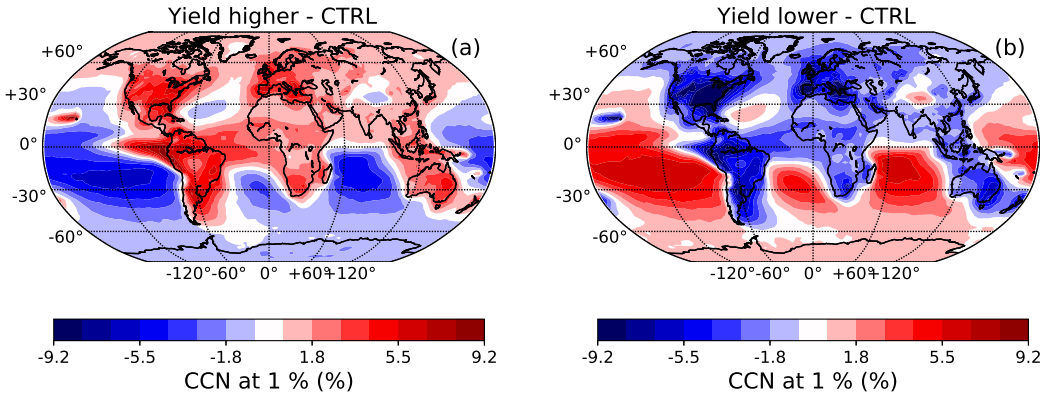

Figure S21. Maps of the difference in annually averaged cloud condensation nuclei at 1% supersaturation between the *Yield higher* and CTRL simulations (a) as well as the *Yield lower* and CTRL simulations (b) for EC-Earth. The CCN concentrations are averaged over for pressures over 850 hPa. The areas close to sources and remote are based on the changes in CCN concentrations in the Yield lower simulation (remote - positive and close to source - negative).